First International Conference on
Bio-based Building Materials

June 22nd - 24th 2015
Clermont-Ferrand, France

3D X-RAY TOMOGRAPHY FOR THE HYGROTHERMAL CHARACTERIZATION OF SPRUCE WOOD

C. El Hachem, K. Abahri*, R. Bennacer

LMT-Cachan UMR 8535, ENS Cachan, Bâtiment Léonard de Vinci, 61 avenue du Président Wilson, 94230 Cachan, France

*Corresponding author; kamilia.abahri@lmt.ens-cachan.fr

Abstract

The bio-based material considered in this work is spruce wood. Because of its complex morphology and high heterogeneity, this material still presents lacks of knowledge, concerning microscopic geometric changes, due to the hygrothermal solicitations. These changes lead usually to a considerable evolution of the resulting thermophysical properties of the material which constrains its use. The swelling and shrinkage phenomena, observed at the macroscopic scale, are the main witnesses reflecting such change caused by the hygric transfer history within the material. Indeed, the latewood/early wood transition present in the wood structure influences substantially the macroscopic behavior of the material, which is strongly dependent on the microscopic one. To answer these questions, a robust identification procedure based on very fine analysis tool is operated. It concerns an experimental investigation based on non-destructive 3D imaging technique "X-ray tomography". This method informs about the three-dimensional microstructure and also allows locating any heterogeneity in the material. The data processing was done using qualitative and quantitative approaches (phase connection, porosity...). Then, successive scans of the same specimen solicited at different hygric states provided the detection of its corresponding water field changes. This step required the development of an original device adapted to the tomograph for imposing constant relative humidity. The obtained results allowed to underscore the swelling phenomenon observed in such materials. In addition, specimens containing a latewood/early wood discontinuity are scanned, and the effect of that discontinuity on the porosity is analyzed.

Keywords:

Spruce wood, X-ray tomography, porosity, 3D microstructure, hygroscopicity, latewood/early wood interface

1 INTRODUCTION

Because of its environmental benefits, spruce wood is widely used in the civil engineering community. It is mainly recommended for inside use. On the other side, many studies, most of which took place at the macroscopic scale, showed that wood's behavior is very sensitive to moisture transfer [Zhou 2000, Anshari 2011]. It is important to note that high moisture content will certainly increase condensation and mould growth risks inside the building envelopes. In addition, this hygroscopic material is subjected to swelling and shrinkage phenomena, even for relative humidity less than 30% [Rafsanjani 2013]. Up than this relative humidity level, the probability of degradation could be easily multiplied. Actually, the wood cells are of a characteristic size of some micrometers. It is thus primordial to deepen the research on the microscopic scale, in order to understand the anisotropy composition of wood which affects its moisture behavior. At this scale, there are many techniques to treat the specimens, but the most non-destructive recommended method used is the X-ray tomography.

Until now, just few researchers were interested on wood's microscopic behavior, as a civil engineering building material. [Trtik 2007] treated spruce wood's microstructural structure, using very small specimens, of dimensions 8x0.2x0.2 mm^3, for which a resolution of 0.7^3 μm^3 was obtained on the tomograph. They were specifically interested in the smallest details in that material, like the pits and the thickness of the fibers. Furthermore, [Mayo 2010] were interested in the topology of many types of wood, as well as comparing early wood and latewood microstructures and porosities. The dimensions of the used samples are 10x2x2 mm^3, 10x1x1 mm^3 and 10x0.5x0.5 mm^3. For the smallest specimens, the resolution obtained was around 1.5^3-2^3 μm^3. Moreover, [Forsberg 2011] made a three-point bending test inside the tomograph with specimen dimensions of 1.57x3.42x0.75 mm^3, for which the resolution was 1.75^3 μm^3. They were interested in the microscopic changes resulting from

the applied mechanical forces. On the other hand, [Li 2013] treated the dynamic evolution of moisture content in many types of wood immersed in water. [Li 2014] studied as well the effect of the layers distribution in plywood on the water resistance. In these last two researches, the dimensions of the used specimens were much bigger than those used in [Trtik 2007], [Mayo 2010] and [Forsberg 2011], and the resolution obtained varied from 7^3 to 100^3 µm^3. In a recent paper, [Gilani 2014] worked on the wood degradation by Physisporinus vitreus and Xylaria longipes. Differences between early wood and latewood for spruce wood and sycamore were treated as well. The dimensions of the specimens used were 1^3 mm^3 and the resolution obtained was 0.7^3 µm^3.

Most of these works neglected the hygric aspect, except those of [Li 2013] and [Li 2014], who worked only on the case of immersion in water. Moreover, the size of the used specimens was too big to reveal the cellular structure of wood, which was not the purpose of their study. In reality, hygrothermal behavior of wood involves complex interactions of different heat, air and moisture transfer mechanisms. At the pore scale, the physical transfer as well as the liquid-vapor interfaces topology, and their interactions with the solid matrix make the study of these mechanisms extremely complex. In fact, the macroscopic material's behavior is highly dependent on the mechanisms involved at the microscopic scale. It is therefore important to make a fine and complete description of the physical process at the microscopic level in order to predict the macroscopic behavior. It is also essential to develop innovative experimental techniques at the microscopic level to face the morphological complexity of the problem and the presence of heterogeneities within materials.

Here, a reliable study of the microstructure of spruce wood is presented. X-ray tomography is used in order to observe the small details in this material. The complicated morphological aspect of this heterogeneous material is treated, by taking into consideration the influence of the latewood/early wood transition on the porosity. In addition, the coupling between the porosity and the moisture state is well considered, by performing tests at dried and controlled relative humidity. A new procedure to get a high resolution in the tomograph, and maintain the same relative humidity during the scans is presented. Using an original method, which is adapted for this kind of material, the porosity and the size distribution of the pores are calculated and analyzed, in order to underscore the swelling phenomena.

2 MATERIAL AND METHODS

In this section, the used wood is introduced, as well as the specimen's protocol preparation. Then, the basic principle of X-ray tomography operation is presented. In order to conserve a constant relative humidity of specimens inside the tomograph during the scan, an adapted device was designed. Finally, the porosity calculation procedure used in this work and adapted for this bio based material is explained.

2.1 Specimen preparation

Spruces are large trees, that exist in the most temperate and boreal regions. Upon age, they grow by reproducing through layering. Each layer represents a cycle in which early wood grows in spring and early summer, followed later by the latewood development [Gilani 2014]. On the microscopic scale, spruce wood is a heterogeneous material that contains vessels, tracheids and pores. At this level, the old cycle ends with latewood cells, and the new one begins with early wood cells. Early wood is characterized by cells having relatively large cavities and thin walls, whereas latewood cells contain smaller cavities and thicker walls [Trechsel 2001]. On the interface that separates two layers, a discontinuity is identified. On the macroscopic scale, the transition from latewood to early wood, which corresponds to the end of a cycle and the beginning of a new one, appears as thick brown fibers, as shown in Fig.1.

Fig. 1: Spruce wood exhibiting many layering cycles through time.

In order to obtain a high resolution in the tomograph, and have access to the material's microstructure, small specimens dimensions were required. In addition, the repeatability of each test was verified, by testing three specimens for each essay, with the same imposed conditions. Moreover, specimens containing the latewood/early wood phase were prepared, in order to quantify wood's anisotropy influence on the porosity. Six spruce wood specimens of dimensions 3x3x20 mm^3 were prepared. The direction of the tracheids was along the 20 mm side. Three of those specimens contained a part corresponding to the latewood/early wood discontinuity. All the scanned samples were without decay, knots and obvious defects. Concerning the protocol of moisture influence on the porosity, the specimens had to be conditioned at maintained relative humidity levels and constant 25°C temperature. Two essential levels were selected: 60% of relative humidity (conditioning room) and dried condition (oven dried at 50°C). The choice of these two distinct relative humidity levels covers sufficiently the hygroscopic zone, and allows quantifying the swelling phenomenon through comparison. Every time a specimen is subjected to new relative humidity conditions, it undergoes microstructural changes, due to the evolution of the water content distribution caused by the sorption phenomenon. For each following moisture stage a regular monitoring of mass sample in time is undertaken until obtaining equilibrium. Once the water content and distribution in a specimen don't evolve anymore, it is considered to have reached its mass equilibrium, and is ready to be scanned. The mass equilibrium depends on the relative mass expression, which is function of the specimen's mass at times t and t-24hours, noted m(t) and m(t-1) respectively, and should verify condition (1) [EN ISO 2001]:

$$\frac{m(t)-m(t-1)}{m(t)} \prec 0.01 \qquad (1)$$

2.2 Adapted X-ray tomography for RH conditioning

All the specimens were scanned with the tomograph X50 at LMT Cachan. X-ray tomography is a non-destructive method, which allows having 3D images of a defined volume. The resolution of those images is function of many parameters, like the distance between the source and the specimen. This parameter is directly related to the dimensions of the specimen. The resolution reached in this case was 3.35x3.35x3.35 μm^3; it is obtained for specimens of 3x3x3 mm^3. With such voxel size, the different heterogeneities in this material could be finely identified, like pores and fibers.

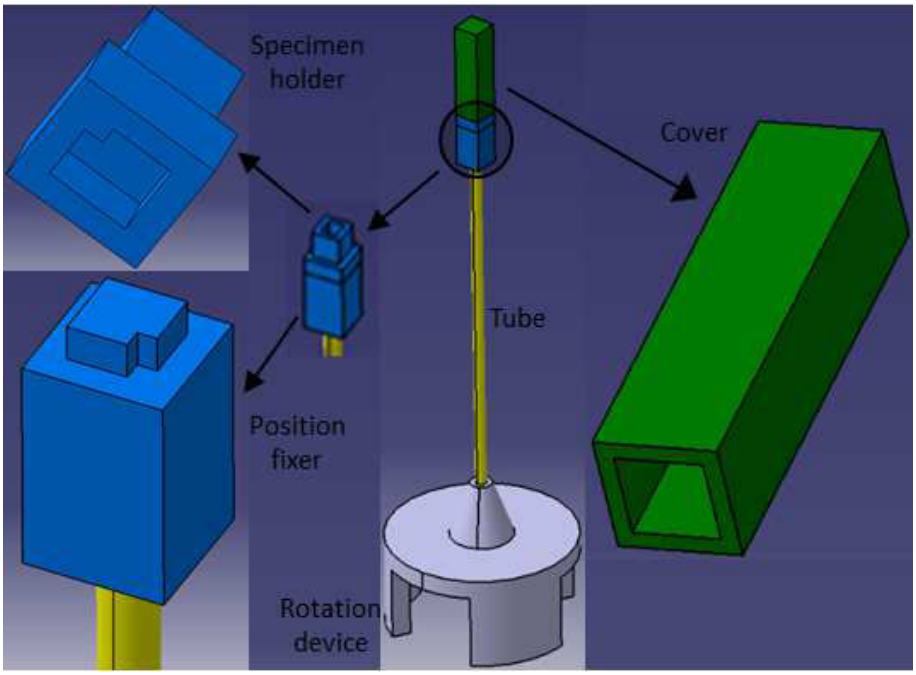

Fig. 2: Device adapted to maintain the sample's conditioning inside the tomograph.

On the other hand, considering that wood is a weakly absorbing material, a special treatment was required to perform imaging scans. After making and analyzing many tests on this material in the tomograph, a choice of using a low voltage of 80 kV and an emission current of 50 µA were selected for all the tests treated in this study. The specimen's size was too small, and each one should conserve its moisture content level during the scan.

Thus, the challenge here was to maintain constant relative humidity conditions for such small dimension of specimens. In addition, another challenge in this study was to refix the specimen at its initial position inside the tomograph, in order to succeed the comparisons protocol between many scans. For that, a new device adapted to X-ray tomography concerning such dimensions of specimens was designed (Fig. 2). It was made using the 3D printer. This device is constituted of a tube attached from one side to the rotation device and from the other side to a piece on which another piece where the specimen was glued should rely inside the tomograph, and a cover. The cover was put inside the conditioning room with the specimen. When the specimen reached its mass equilibrium, it was covered inside the conditioning room, and taken inside the tomograph to be scanned. That way, the specimen should remain in the same humidity atmosphere while scanning, and the transfers were minimized as much as possible.

2.3 Porosity calculation procedure

After each scan, the reconstruction was made using the software efX, and the volume was treated on ImageJ [Schneider 2012]. Each reconstructed volume contains many pixels in each direction. A voxel is defined as 1x1x1 $pixel^3$. A value which is function of the density of the voxel content is assimilated to each voxel. The next step is to apply a threshold to the volume. In this step, a function φ(solid matrix) or φ(air) is assimilated to each voxel, depending on whether it represents the solid matrix or the air. φ(solid matrix) has a value of 0 and φ(air) has a value of 1. The conventional porosity represented in equation (2), is defined as the ratio between the voxels for which a value of 1 was assigned and the total voxels inside the volume, as following:

$$P=\int_x\int_y\int_z \varphi(\text{air})\,dxdydz \quad (2)$$

In this work, a local porosity which corresponds to a specific direction is defined as well.

It represents the surface porosity of a section. The local porosity in x, y and z directions are presented in equations (3), (4) and (5), respectively. Each equation is valid for a specific x, y and z value respectively:

$$P(x)=\int_y\int_z \varphi(\text{air})\,dydz \quad (3)$$

$$P(y)=\int_x\int_z \varphi(\text{air})\,dxdz \quad (4)$$

$$P(z)=\int_x\int_y \varphi(\text{air})\,dxdy \quad (5)$$

Hence, later in this paper, the porosity evolution in each direction is represented in a graph showing the local porosity calculated perpendicular to the considered axis, and function of the position along the direction in question.

Many volume treatments were performed on ImageJ because of the cumbersome process. Firstly, the preliminary reconstructed volume contained the specimen, as well as the air around it. Therefore, it

was necessary to crop the volume in the 3 directions, to eliminate the parts that don't belong to the specimen. For all the samples, the same size was cropped, which corresponded to the **R**egion **O**f **I**nterest (**ROI**). The dimensions of the ROI selected were 500x500x500 pixels^3, which was equivalent in these tests to 1.65x1.65x1.65 mm^3. Great comparisons could be made, because of the ability to maintain approximately the same position of the ROI for different relative humidity conditions. Secondly, in order to make the comparison for a specimen, between two relative humidity levels, it was very important to calculate the pore size distribution, as well as the porosity itself, at each level. Finally, it was also important for many purposes, to see the evolution of the porosity along the three axis x, y and z, with z the axis perpendicular to the images and parallel to the tracheid direction, and x and y the axis in the plane corresponding to an image. In order to do all these treatments, the ImageJ plugins of [Maire 2007] were used.

3 RESULTS AND DISCUSSION

Wood is a multiphase material. It contains air, liquid water and vapor. Unfortunately, water is hierarchically distributed inside. Hence, it is essential to use a powerful procedure in order to distinguish these phases and how this water interacts with the material solid matrix. Fig. 3 and Fig. 4 represent a scanned specimen without the latewood/early wood interface, at dry conditions, in a 3D view and in the (x,y) plane respectively. It is important to mention that the 3D view was reconstructed using efX software and corresponds to the whole specimen, before making a crop of the ROI.

The resolution of 3.35^3 µm^3 obtained on the tomograph, was sufficient to distinguish the different heterogeneities of this material. The fibers, which form the tracheids and the vessels, were easily identified, as well as the pores. It is evident in these images that for such a material, each tracheid corresponds actually to a representative elementary cell, which is obviously periodic in the (x,y) plane. Moreover, the cells repartition looks like it tends to verify a certain alignment along the (x,y) plane. This cell has a specific direction along the z axis. Because of its shape and direction, it can be assimilated to a microscopic tunnel. It is evident that in such microstructure, the hygric transfer in this material can favor a direction among others. For example, in that case, the transfers kinetic toward z direction are surely faster than the ones toward x and y directions.

The evolution of the porosity in z direction of a dried specimen is presented in Fig. 5. The porosity calculated for this specimen was 65%. Concerning the porosity in the z direction, each point in the curve represents a porosity value in the corresponding plane (x,y) where each (x,y) plane corresponds to an image. Concerning the z direction, there was no big fluctuations between two successive positions, which was a proof of the fiber continuity along the thickness of the specimen. In addition, the standard deviation of the porosity along the z axis was less than 0.5%, which is a sign of the images morphological similarity.

3.1 Interface discontinuity influence

The ROI of a dried specimen containing the latewood/early wood discontinuity is represented in Fig. 6 and Fig. 7, in a 3D view on ImageJ and in (x,y) plane respectively. In both figures, it can be observed that the latewood phase is characterized by the cells containing thicker walls and smaller cavities that become smaller when approaching the latewood/early wood interface. It is remarkable as well that the smallest pores belong to the thickest fibers. After zooming on the discontinuity phase in Fig. 7, it is obvious that the smallest size of pores can be even smaller than a pixel, which means smaller than 3.35 µm.

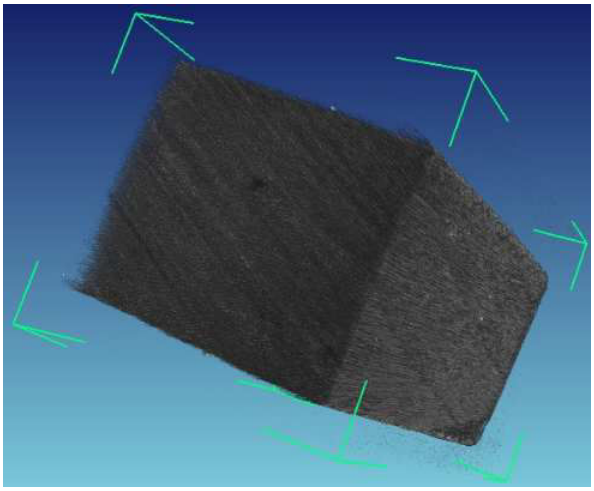

Fig. 3: 3D reconstruction of a specimen of dimensions 3x3x3 mm^3 with a resolution of 3.35x3.35x3.35 µm^3 at dried conditions before cropping the ROI.

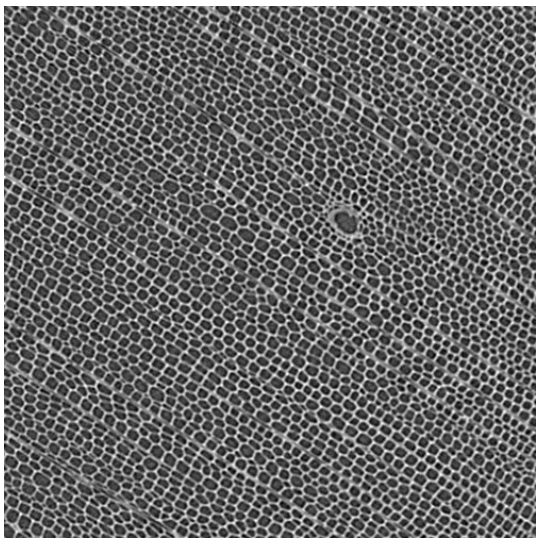

Fig. 4: ROI of a dried specimen in the (x,y) plane.

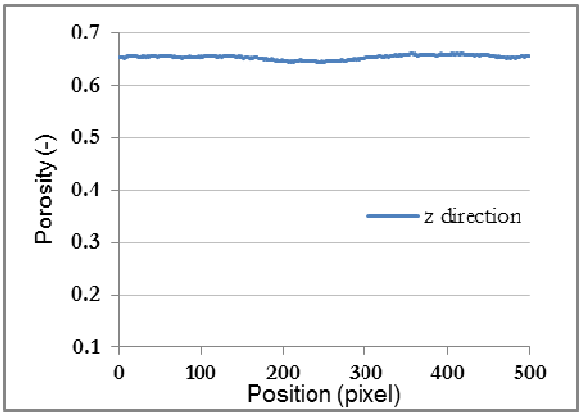

Fig. 5: Evolution of the porosity of a dried specimen along the z direction.

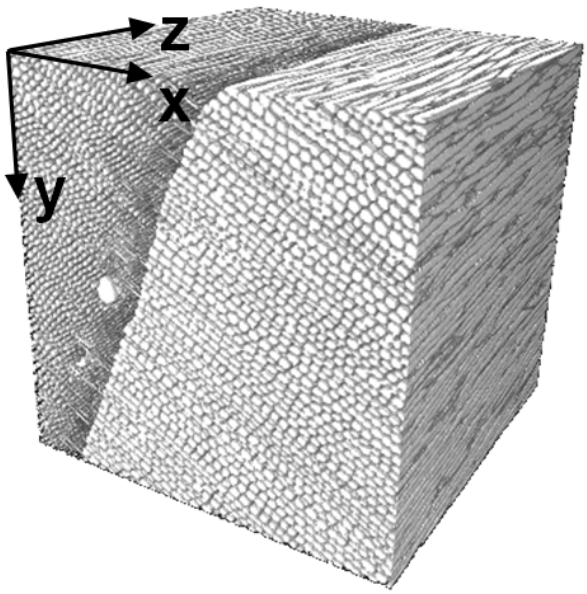

Fig. 6: A 3D view on ImageJ of the ROI of a dried specimen with the latewood/early wood transition.

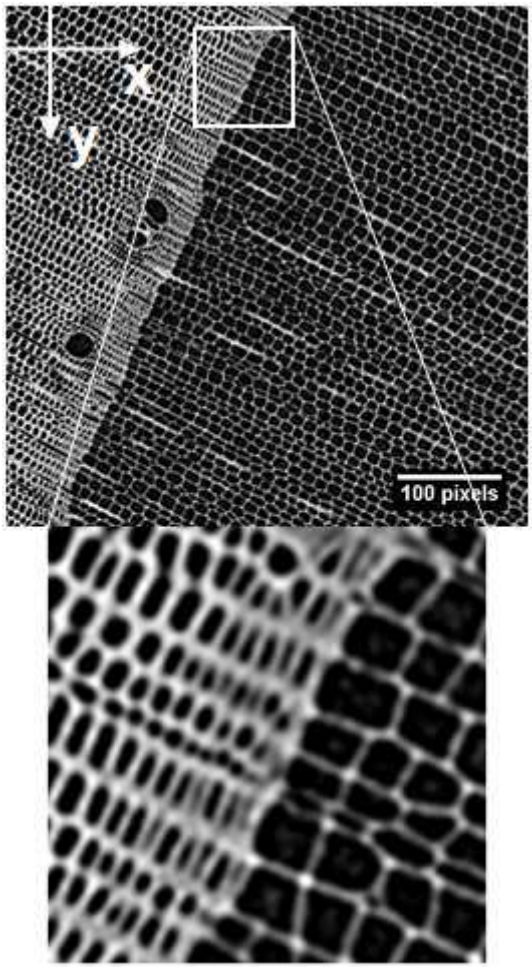

Fig. 7: ROI of a dried specimen with the latewood/ early wood transition in the (x,y) plane, and a zoom on the transition.

For this specimen, the calculated porosity is 69%. For better evaluation of the influence of the latewood/early wood anisotropy on the specimen's porosity, it was important to observe the evolution of the porosity along the x and y directions (Fig. 8).

It is obvious that along the z axis, the variability of the porosity is similar to that showed in Fig. 5, which corresponds to a specimen without latewood/early wood phases. Hence, the parallel sections along the tracheids direction are also similar.

Fig. 6 and Fig. 7 show that the latewood phase is much thicker at the top than in the bottom, which can be observed in the curve showing the porosity evolution in y direction (Fig. 8). The left and right porosity values of this curve are respectively 64% and 73%. This result shows that along the y axis, the porosity increases when the thickness of the latewood phase decreases.

Concerning the x direction, the result is much more evident. Actually, in the phase corresponding to the latewood only, the porosity is approximately 50%. On the other hand, in the phase corresponding to the early wood only, the porosity is approximately 80%. The porosity corresponding to the latewood/early wood transition varies from 50 to 80%.

As a conclusion, the presence of the latewood/early wood discontinuity in the material decreases its porosity. In addition, for a random specimen, regardless of the material phase to which it belongs, its porosity can vary from 50% to 80%.

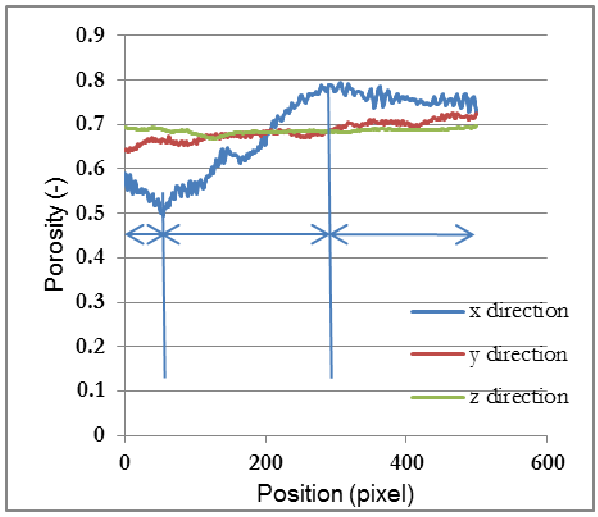

Fig. 8: Evolution of the dried specimen's porosity with the latewood/ early wood discontinuity in x, y and z directions.

3.2 Swelling analysis

In this part, the swelling due to hygric solicitations is investigated. Images of a specimen that doesn't contain a latewood/early wood discontinuity, at dried and controlled relative humidity conditions, are presented in Fig. 9. Comparing these two images, it appears that the specimen has swollen because of adsorption phenomenon, which affected its morphology. In order to well underscore this phenomenon, the distance between two irregularities in the specimen is calculated at the same position (before and after adsorption), as shown in Fig. 9. The distances calculated for the dried and controlled conditions are respectively 331.8 pixels and 336.4 pixels. Considering that each pixel represents 3.35 µm, those distances correspond to 1111 µm and 1130 µm respectively. This difference represents a deformation of 1.7%.

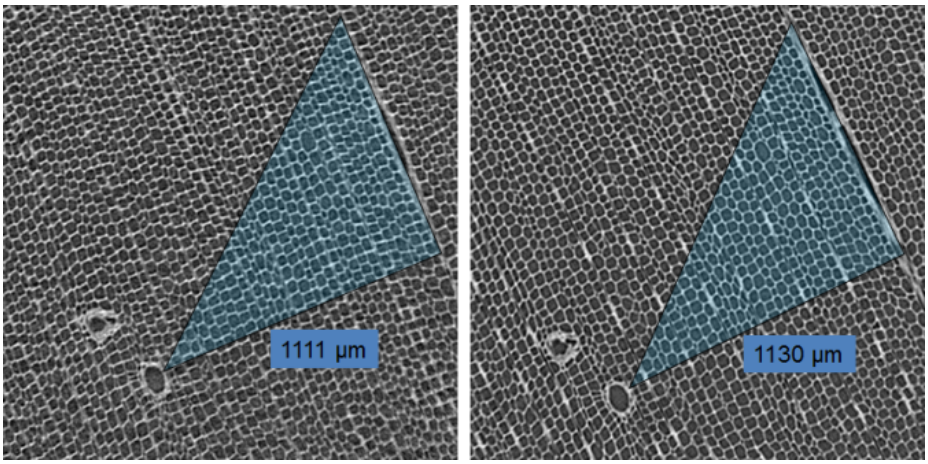

Fig. 9: ROI of a specimen at dried (left) and fixed (right) relative humidity conditions, with calculated distances between two irregularities for both cases.

Another way to underscore the swelling phenomenon is to use the plugins developed by [Maire 2007], which calculate the distribution of the radiuses of the pores in the volume. Therefore, by applying this plugin to the same specimen at both relative humidity conditions, the pores radiuses distribution can be observed in Fig. 10. What is evident in this figure is that for both relative humidity conditions, the majority of the pores have a radius of 10 pixels. In addition, for a relative humidity of 60%, the distribution of the radiuses of the pores contains much bigger pores, and much less smaller pores than the dried case.

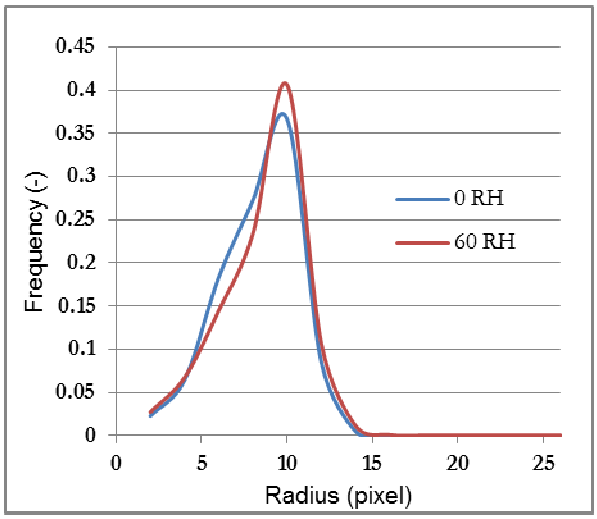

Fig.10: Distribution of radiuses of the pores for a specimen at dried and fixed conditions.

On the other hand, local porosities of 65% and 61% are calculated respectively for dried and fixed relative humidity levels. The porosity evolution in z direction for both cases is represented in Fig. 11. This result is evident, considering that the water content in the specimen increases for higher relative humidity state, which leads to a decreasing porosity.

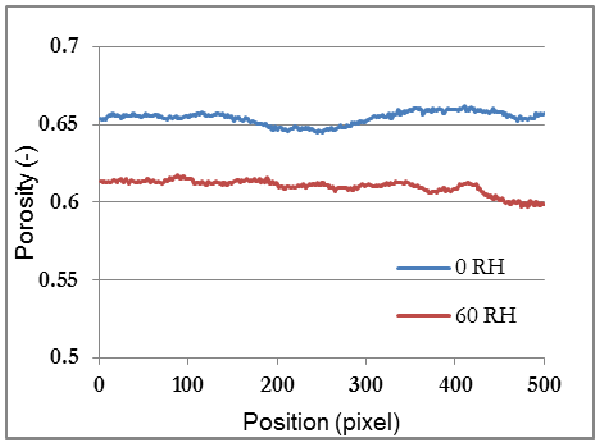

Fig. 11: Evolution of the specimen's porosity in z direction, at dried and controlled conditions.

4 CONCLUSION

In the present paper, a non-destructive 3D imaging technique X-ray tomography on spruce wood has been investigated. The wood's microstructure and its anisotropy composition had been identified and presented with a resolution of 3.35^3 µm^3. The imaging scans treatment reveals that transfers can be favored in the tracheids direction among other directions. In addition, the results show that the latewood/early wood discontinuity tends to decrease the porosity of the material, considering that the porosity between the latewood and early wood varies from 50% to 80%.

In order to examine the hygric solicitations effects on this hygroscopic material, an adapted X-ray tomography device was constructed for the microscopic dimensions of the used specimens. In addition to its ability to maintain a constant relative humidity inside the tomograph, this device conserves the specimen's position from a scan to another. Results show that when a specimen passes from to 0 to 60% relative humidity, its porosity decreases. Moreover, the specimen is subjected to a swelling phenomenon, which is underscored by the bigger size of pores at the 60% relative humidity conditions. This paper contains many promising results, concerning the microscopic morphological study of spruce wood, and its sensitivity to the hygric solicitations. For further work, it would be desirable to extend this study in order to identify the real cause of the observed swelling phenomenon covering the whole hygroscopic range.

5 REFERENCES

[Anshari 2011] Anshari, B.; Guan, Z.W.; Kitamori, A.; Kung, A. et al.; Mechanical and moisture-dependent swelling properties of compressed Japanese cedar. Construction and Building Materials, 2013, 25, 1718-1725.

[EN ISO 2001] Hygrothermal performance of building materials and products - Determination of hygroscopic sorption properties, ISO12571, 2001.

[Forsberg 2010] Forsberg, F.; Sjödahl, M.; Mooser, R.; Hack, E. et al.; Full Three-Dimensional Strain Measurements on Wood Exposed to Three-Point Bending: Analysis by Use of Digital Volume Correlation Applied to Synchrotron Radiation Micro-Computed Tomography Image Data. Strain, 2010, 46, 47-60.

[Gilani 2014] Gilani, M.S.; Boone, M.S.; Mader, K.; Schwarze, F.W.M.R.; Synchrotron X-ray micro-tomography imaging and analysis of wood degraded by Physisporinus vitreus and Xylaria longipes. Journal of Structural Biology, 2014, 187, 2, 149-157.

[Li 2013] Li, W.; Bulcke, J.V.; Windt, I.D.; Loo, D.V. et al.; Combining electrical resistance and 3-D X-ray computed tomography for moisture distribution measurements in wood products exposed in dynamic moisture conditions. Building and Environment, 2013, 67, 250-259.

[Li 2014] Li, W.; Bulcke, J.V.; Mannes, D.; Lehmann, E. et al.; Impact of internal structure on water-resistance of plywood studied using neutron radiography and X-ray tomography. Construction and Building Materials, 2014, 73, 171-179.

[Maire 2007] Maire, E.; Colombo, P.; Adrien, J.; Babout, L. et al.; Characterization of the morphology of cellular ceramics by 3D image processing of X-ray tomography. Journal of the European Ceramic Society, 2007, 27, 1973-1981.

[Mayo 2010] Mayo, S.C.; Chen, F.; Evans, R.; Micron-scale 3D imaging of wood and plant microstructure using high-resolution X-ray phase-contrast microtomography. Journal of Structural Biology, 2010, 171, 2, 182-188.

[Ranfsanjani 2013] Ranfsanjani, A.; Lanvermann, C.; Niemz, P.; Carmeliet, J. et al.; Multiscale analysis of free swelling of Norway spruce. Composites: Part A, 2013, 54, 70-78.

[Schneider 2012] Schneider, C.A.; Rasband, W.S.; Eliceiri, K.W.; NIH Image to ImageJ: 25 years of image analysis. Nature Methods, 2012, 9, 671-675.

[Trtik 2007] Trtik, P.; Dual, J.; Keunecke, D.; Mannes, D. et al.; 3D imaging of microstructure of spruce wood. Journal of Structural Biology, 2007, 159, 1, 46-55.

[Trechsel 2001] Trechsel, H.R.; Moisture Analysis and Condensation Control in Building Envelopes, ISBN 9780803120891, ASTM International, 2001.

[Zhou 2000] Zhou, Y.; Fushitani, M.; Sato, K.; Ozawa, M.; Bending creep behavior of hot-pressed wood under cyclic moisture change conditions. Journal of wood science, 2000, 46, 423-430.